Scale-Invariant Dynamics of Galaxies, MOND, Dark Matter, and the Dwarf Spheroidals

Andre Maeder [1]⋆ and Vesselin G. Gueorguiev [2,3]†

[1]*Geneva Observatory - chemin des Maillettes 51, CH-1290 Sauverny, Switzerland*
[2]*Institute for Advanced Physical Studies - 21 Montevideo Street, Sofia 1618, Bulgaria*
[3]*Ronin Institute for Independent Scholarship - 127 Haddon Pl., Montclair, NJ 07043, USA*

ABSTRACT

The Scale-Invariant Vacuum (SIV) theory is based on Weyl's Integrable Geometry, endowed with a gauge scalar field. The main difference between MOND and the SIV theory is that the first considers a global dilatation invariance of space and time, where the scale factor λ is a constant, while the second opens the likely possibility that λ is a function of time. The key equations of the SIV framework are used here to study the relationship between the Newtonian gravitational acceleration due to baryonic matter g_{bar} and the observed kinematical acceleration g_{obs}. The relationship is applied to galactic systems of the same age where the Radial Acceleration Relation (RAR), between the g_{obs} and g_{bar} accelerations, can be compared with observational data. The SIV theory shows an excellent agreement with observations and with MOND for baryonic gravities $g_{\mathrm{bar}} > 10^{-11.5}$ m s^{-2}. Below this value, SIV still fully agrees with the observations, as well as with the horizontal asymptote of the RAR for dwarf spheroidals, while this is not the case for MOND. These results support the view that there is no need for dark matter and that the RAR and related dynamical properties of galaxies can be interpreted by a modification of gravitation.

Key words: Galaxies: rotation – Cosmology: theory – dark matter

1 INTRODUCTION

The Scale-Invariant Vacuum (SIV) theory is based on the Weyl Integrable Geometry. A general scale-invariant field equation and a geodesic equation have been obtained first by Dirac (1973) and Canuto et al. (1977) and their consistency as a framework for gravitation and the motion of astronomical bodies have been further developed by Bouvier & Maeder (1978).

"It appears as one of the fundamental principles in Nature that the equations expressing basic laws should be invariant under the widest possible group of transformations" (Dirac 1973). The scale or gauge invariance of physical laws is a fundamental property in physics. Maxwell's equations are scale-invariant in the empty space, this is also true for General Relativity (GR) if the cosmological constant Λ_{E} is absent. Scale invariance means that the equations do not change for a transformation of the line element of the form,

$$ds' = \lambda(t)\,ds\,, \tag{1}$$

where ds' is the line element of GR and ds the line element of a more general space where scale invariance is also present. The term $\lambda(t)$ is the scale factor. It is considered to not depend on space for reason of homogeneity and isotropy. The requirement of scale invariance in addition to the general covariance implies to move from the Riemann Geometry to Weyl's Geometry, which in addition to a metric form $ds^2 = g_{\mu\nu}dx^\mu dx^\nu$ is endowed with a scalar field Φ (see Equation 7 below). By adding the gauging condition that the macroscopic empty space is scale-invariant, the corresponding general scale-invariant field and geodesic equations obtained by Canuto et al. (1977) have been applied successfully to several basic cosmological tests (Maeder 2017a), to clusters of galaxies and galactic properties (Maeder 2017c), as well as to the growth of density fluctuations in the early Universe (Maeder and Gueorguiev 2019).

The astrophysical problem considered here, within the scale-invariant framework as well as in the context of MOND, concerns the Radial Acceleration Relation (RAR) of galaxies. The RAR compares the centripetal acceleration g_{obs}, traced by the rotation curves of spiral galaxies, and the expected gravitational acceleration due to the observed distribution of baryons g_{bar} (McGaugh 2004; McCaugh et al. 2016; Lelli et al. 2017; Li et al. 2018). Below a gravity of

⋆ E-mail: andre.maeder at unige.ch
† E-mail: vesselin.gueorguiev at ronininstitute.org

about 10^{-10} m s^{-2}, the RAR deviates from the 1:1 line, g_{obs} being much larger than g_{bar}. The RAR is followed by late and early type galaxies, and also by the dwarf spheroidals where the deviations from the 1:1 line are the largest ones.

These deviations are currently attributed to dark matter. Lelli et al. (2017) point out that the dark matter distribution is fully determined by that of the baryons or vice-versa. A number of authors have interpreted this relation in the context of the ΛCDM models of galaxy formation, in terms of different mass-dependent density profiles of DM haloes (Di Cintio and Lelli 2016), of simulations of galaxy formation matching the velocities and the scaling relations (Santos-Santos 2016), in particular if stellar masses and sizes are closely related to the masses and sizes of their DM haloes (Navarro et al. 2017; Desmond 2017). Keller and Wadsley (2017) show that the account for the hot outflows from supernovae at high z improves the comparisons by producing a baryon depletion, while the effects of the AGN feedback is considered by Ludlow et al. (2017).

Attempts to explain the RAR in the context of modified gravity (MOND) have been successfully made by Milgrom (2016) and Li et al. (2018). The MOND theory (Milgrom 1983, 2009) shows some significant successes in explaining galactic properties, such as the flat rotation curves of spiral galaxies, the radial acceleration relation (RAR) of galaxies (McCaugh et al. 2016; Lelli et al. 2017), and the Tully-Fisher relation. Its mutual advantages and disadvantages with respect to the current ΛCDM model have been analyzed by McGaugh (2015). The MOND theory also presents some properties of coordinate scale invariance (Milgrom 2009, 2014), such that

$$(t, \mathbf{r}) \rightarrow (\lambda\, t, \lambda \mathbf{r}), \tag{2}$$

where here λ is a constant term. This is a global dilatation invariance independent on time and space, much less constraining than a scale invariance to a transformation like in equation (1). Thus, the main difference between MOND and SIV theory is that the first does not consider a possible time variation of the scale factor λ, while the second allows this possibility. This makes a big difference because the first and second derivatives of λ will appear in the dynamical equations. In this context, it is interesting to investigate the possible relation, if any, between MOND and the SIV framework (Maeder 2017a) that rests on a more general time-dependent scale invariance.

In this work, new research lines are explored, a justified objective, especially in the present context, where the dominant mass-energy source is unknown. In Section 2, we summarize the main relevant properties of the Integrable Weyl Geometry which serves as a basis for further developments. In Section 3, we express the field and geodesic equations, as well as the adopted gauge condition. Section 4 applies the weak-field equation and derives the relation between the kinematic rotational acceleration and the baryonic matter present. Section 5 presents the comparison of the results with observations and compares to the MOND predictions. Section 6 is devoted to the conclusion summary.

2 KEY EQUATIONS OF THE INTEGRABLE WEYL'S GEOMETRY

Weyl's Geometry is a generalization of the Riemann Geometry first proposed by Hermann Weyl (Weyl 1923) and further developed by Eddington (1923) and Dirac (1973). Weyl's Geometry is the appropriate framework to study scale invariance problems, in particular the corresponding Integrable Weyl's Geometry Canuto et al. (1977) and Bouvier & Maeder (1978). In addition to the general covariance of GR, it considers gauge or scale transformations. The original aim of Weyl was to interpret the electromagnetism in terms of properties of the space-time geometry, as Einstein did for gravitation. This geometry is endowed with a metrical determination of the quadratic form $ds^2 = g_{\mu\nu}(x)dx^\mu dx^\nu$ as in Riemann space, and with quantities expressing gauge transformations. Let us consider a vector of length ℓ attached at a point P of coordinates x^μ. If this vector is transported by parallel displacement to a point P' of coordinates $x^\mu + \delta x^\mu$, its length becomes $\ell + \delta\ell$, where

$$\delta\ell = \ell \kappa_\mu \delta x^\mu \,, \tag{3}$$

where κ_μ is called the coefficient of metrical connection. In Weyl's geometry, terms κ_μ are fundamental coefficients as are the $g_{\mu\nu}$ in GR. The lengths undergo corresponding gauge changes:

$$\ell' = \lambda(x)\ell \,, \tag{4}$$

where λ is the scale gauge factor, which could in principle depend on the 4–coordinates. The segment $\delta\ell'$ also changes. To the first order in δx^ν, one has:

$$\ell' + \delta\ell' = (\ell + \delta\ell)\lambda(x + \delta x) = (\ell + \delta\ell)\lambda(x) + \ell\frac{\partial\lambda}{\partial x^\nu}\delta x^\nu, \tag{5}$$

$$\begin{aligned}\delta\ell' &= \lambda\,\delta\ell + \ell\lambda_{,\nu}\delta x^\nu = \lambda\ell\kappa_\nu\delta x^\nu + \ell\lambda_{,\nu}\delta x^\nu = \\ &= \lambda\ell(\kappa_\nu + \Phi_{,\nu})\delta x^\nu = l'\kappa'_\nu\delta x^\nu,\end{aligned} \tag{6}$$

where the notation $\lambda_{,\nu} = \frac{\partial\lambda}{\partial x^\nu}$ is used along with:

$$\Phi = \ln\lambda\,, \quad\text{and}\quad \kappa'_\nu = \kappa_\nu + \Phi_{,\nu} = \kappa_\nu + \partial_\nu\ln\lambda\,. \tag{7}$$

If the vector is parallel transported along a closed loop, the total change of the length of the vector can be written as:

$$\Delta\ell = \ell\left(\partial_\nu\kappa_\mu - \partial_\mu\kappa_\nu\right)\sigma^{\mu\nu}\,, \tag{8}$$

where $\sigma^{\mu\nu} = dx^\mu \wedge dx^\nu$ is an infinitesimal surface element corresponding to the edges dx^μ and dx^ν. The tensor $F_{\mu\nu} = \left(\kappa_{\mu,\nu} - \kappa_{\nu,\mu}\right)$ was identified by Weyl with the electromagnetic field. However, in the above form of the Weyl's geometry, the lengths are non-integrable: the change of the length of a vector between two points depends on the path considered. Such a property would imply that different atoms, due to their different world lines, would have different properties and thus will emit at different frequencies. This was the essence of Einstein's objection against Weyl's geometry, as recalled by Canuto et al. (1977).

The above objection does not hold if one considers the so-called Integrable Weyl's Geometry, which forms a consistent framework for the study of gravitation as emphasized by Canuto et al. (1977) and Bouvier & Maeder (1978). Let us consider that the framework of functions denoted by primes

is the Riemann space as in GR. That is, $\kappa'_\nu = 0$, and therefore:

$$\kappa_\nu = -\Phi_{,\nu} = -\frac{\partial \ln \lambda}{\partial x^\nu}. \qquad (9)$$

The above condition means that the metrical connection κ_ν is the gradient of a scalar field ($\Phi = \ln \lambda$), as seen above. Thus, $\kappa_\nu dx^\nu$ is an exact differential and therefore:

$$\partial_\nu \kappa_\mu = \partial_\mu \kappa_\nu, \qquad (10)$$

which according to Equation (8) implies that the parallel displacement of a vector along a closed loop does not change its length, equivalently the change of the length due to a displacement does not depend on the path followed. Many mathematical tools of Weyl's geometry also work in the integrable form of this geometry. The line element $ds' = g'_{\mu\nu} dx^\mu dx^\nu$ refers to GR, while ds in Equation (1) refers to the Integrable Weyl Geometry, which is also endowed with a scalar gauge field Φ.

The integrable Weyl's space is conformally equivalent to a Riemann space (pseudo-space) defined by $g'_{\mu\nu}$ with $\kappa'_\nu = 0$ via the λ mapping which represents gauge re-scaling:

$$g'_{\mu\nu} = \lambda^2 g_{\mu\nu}. \qquad (11)$$

Such conformal mappings have been related to space-time deformations and have been studied in connection with a large class of Extended Theories of Gravity (Capozziello & Stornaiolo 2008; Capozziello & de Laurentis 2011). When the traceless symmetric and antisymmetric components of these general transformations are absent the corresponding generalized conformal transformations become simple conformal mappings. In this respect, Eq. (11) relates the original unmodified metrics and the "deformed metrics" of the scale-invariant vacuum space-time. According to Capozziello & Stornaiolo (2008), the space-time deformations act like a force that deviates the test particles from the unperturbed motions and these authors also express the corresponding geodesics and general field equation that are consistent with Canuto et al. (1977) and Bouvier & Maeder (1978).

The conformal factor that is only time dependent is an important ingredient in the SIV theory since it allows space-time deformations that obey the cosmological principle and keep the space homogenous and isotropic at every moment of time. If λ is to depend on the space coordinates, i.e, as in Brans-Dicke theory of gravity, then one would face such undesirable inhomogeneity problems. Furthermore, due to the Universality of the Einstein theory of gravitation (Kijowski 2016), any Extended Theories of Gravity can be put into an equivalent standard GR theory with (possibly) a different metric tensor plus (possibly) a different set of matter fields. There could be at least one effective scalar field as in Brans-Dicke theory. Here, this scalar field is that expressed by the metrical connection κ_ν. Furthermore, we may remark that in the scale-invariant vacuum theory the "deformation" is not necessarily a perturbation of the standard motion, it can even become the dominant effect as illustrated by the scale-invariant cosmological models (Maeder 2017a) which show that the accelerated expansion becomes the leading term in

the advanced evolutionary stages of the Universe. An interesting case of Extended Theories of Gravity is the case of the "$f(R)$- theory of Gravity" (Capozziello et al. 2006), where the Lagrangian contains some function $f(R)$ of the Ricci curvature scalar R (instead of just R). Such theories have been developed and also applied to the dynamics of spiral and elliptical galaxies by Capozziello et al. (2017) and will be further discussed in Section 5.4.

In the framework of Weyl's Geometry, scalars, vectors, or tensors that transform like

$$Y'^\nu_\mu = \lambda^n Y^\nu_\mu, \qquad (12)$$

are respectively called co-scalars, co-vectors, or co-tensors of power n. If $n = 0$, one has an in-scalar, in-vector or in-tensor, such objects are invariant upon a scale transformation. Scale covariance refers to a transformation with powers n different from zero, while the term scale invariance is generally reserved for cases with $n = 0$. On the basis of the properties recalled above, a so-called cotensor analysis has been developed (Weyl 1923; Eddington 1923; Dirac 1973; Canuto et al. 1977). Bouvier & Maeder (1978) have also derived the equation of geodesics from an action principle and shown its consistency with the notion of the shortest distance between two points, they have also reviewed the notion of parallel displacement, of isometries and Killing vectors in the Integrable Weyl's Geometry. In general, the derivative of a scale-invariant object is not scale invariant. Thus, scale covariant derivatives of the first and second order have been developed preserving scale covariance. For example, the co-covariant derivatives $A_{\mu*\nu}$ and $A^\mu_{*\nu}$ of a co-vector A_μ of power n are:

$$A_{\mu*\nu} = \partial_\nu A_\mu - {}^*\Gamma^\alpha_{\mu\nu} A_\alpha - n\kappa_\nu A_\mu, \qquad (13)$$

$$A^\mu_{*\nu} = \partial_\nu A^\mu + {}^*\Gamma^\mu_{\nu\alpha} A^\alpha - n\kappa_\nu A^\mu, \qquad (14)$$

$$\text{with} \quad {}^*\Gamma^\alpha_{\mu\nu} = \Gamma^\alpha_{\mu\nu} + g_{\mu\nu}\kappa^\alpha - g^\alpha_\mu \kappa_\nu - g^\alpha_\nu \kappa_\mu. \qquad (15)$$

Here ${}^*\Gamma^\alpha_{\mu\nu}$ is a modified Christoffel symbol, while $\Gamma^\alpha_{\mu\nu}$ is the usual Christoffel symbol. For more details on the cotensor calculus, the interested reader may read Chapter VII of "The Mathematical Theory of Relativity (Eddington 1923), as well as Dirac (1973). We also point out that Canuto et al. (1977) provided a short summary of the cotensor analysis. In this framework, the Riemann curvature tensor $R^\nu_{\mu\lambda\rho}$, its contracted form, the Ricci tensor R^ν_μ, and the scalar curvature R also have their corresponding scale-covariant expressions:

$$R^\nu_\mu = R'^\nu_\mu - \kappa^{;\nu}_\mu - \kappa^\nu_{;\mu} - g^\nu_\mu \kappa^\alpha_{;\alpha} - 2\kappa_\mu \kappa^\nu + 2g^\nu_\mu \kappa^\alpha \kappa_\alpha. \qquad (16)$$

$$R = R' - 6\kappa^\alpha_{;\alpha} + 6\kappa^\alpha \kappa_\alpha. \qquad (17)$$

Here the terms with a prime are the usual expressions in the Riemann geometry, and the semicolon ' ; ' indicates the usual covariant derivative with respect to the relevant coordinate.

The main difference with the standard tensor analysis is that all these expressions contain terms depending on the additional scalar field through the coefficient of metrical connection κ_ν given by the above Equation (9). We notice that the curvature term has been modified as is the case in the context of the "Extended Theories of Gravity" (Capozziello & de Laurentis 2011).

3   THE SCALE-INVARIANT EQUATIONS FOR THE METRIC AND THE GAUGE FIXING

The above developments of the equivalent expressions of the Ricci tensor and curvature scalar lead to the expression of the general field equation. We note that it can also be obtained by using the properties of conformal equations for the Ricci tensor and curvature scalar, as well as by the application of an action principle, as shown by Canuto et al. (1977). The field equation is

$$R'_{\mu\nu} - \frac{1}{2}\,g_{\mu\nu}R' - \kappa_{\mu;\nu} - \kappa_{\nu;\mu} - 2\kappa_\mu\kappa_\nu + 2g_{\mu\nu}\kappa^\alpha_{;\alpha} - g_{\mu\nu}\kappa^\alpha\kappa_\alpha =$$
$$= -8\pi G T_{\mu\nu} - \lambda^2\Lambda_E\,g_{\mu\nu}\,, \quad (18)$$

where G is the gravitational constant (taken here as a true constant) and Λ_E the Einstein cosmological constant. The energy-momentum intensor $T_{\mu\nu}$ must be a scale-invariant quantity, as is the first member of the scale-invariant field equation, *i.e.* $T_{\mu\nu} = T'_{\mu\nu}$. This requirement has some important implications for pressures and densities (Canuto et al. 1977). Expressing this condition, one has:

$$(p+\rho)u_\mu u_\nu - g_{\mu\nu}p = (p'+\rho')u'_\mu u'_\nu - g'_{\mu\nu}p'\,. \quad (19)$$

The four-velocities u'^μ and u'_μ transform like a co-vector of order ∓ 1:

$$u'^\mu = \frac{dx^\mu}{ds'} = \lambda^{-1}\frac{dx^\mu}{ds} = \lambda^{-1}u^\mu,$$
$$u'_\mu = g'_{\mu\nu}u'^\nu = \lambda^2 g_{\mu\nu}\lambda^{-1}u^\nu = \lambda\,u_\mu\,. \quad (20)$$

Thus, from the expression of the energy-momentum intensor the transformations for p and ρ follow:

$$(p+\rho)u_\mu u_\nu - g_{\mu\nu}p = (p'+\rho')\lambda^2 u_\mu u_\nu - \lambda^2 g_{\mu\nu}p'\,, \quad (21)$$
$$\Rightarrow p = p'\lambda^2 \text{ and } \rho = \rho'\lambda^2\,. \quad (22)$$

The pressure and density are therefore not scale-invariant, but are so-called co-scalars of power $n = -2$. A similar scaling appears for the term containing the cosmological constant, $-\lambda^2\Lambda_E\,g_{\mu\nu}$; thus, Λ_E is also a co-tensor of power $n = -2$ since $\lambda^2\Lambda'_E = \Lambda_E$. The product $\lambda^2\Lambda_E$, as it stands in the field equation (18), is evidently gauge invariant (in-scalar) and thus we have a consistent scale-invariant field equation containing a non-zero cosmological constant. The best way to see this is to consider the in-scalar equations (18) with one contra-variant and one covariant index (upper and lower) that are gauge invariant, thus requiring $\lambda^2\Lambda_E$ to be gauge invariant as well. Here, it is an opportunity to recall the remark by Bondi (1990), who pointed out that "Einstein's disenchantment with the cosmological constant was partially motivated by a desire to preserve scale-invariance of the empty space Einstein equations".

The field equation (18) is undetermined due to the gauge symmetry of the equations and the same remark applies to the resulting differential equations either in cosmology or for the Newton-like approximation. The same problem appears in General Relativity, where the under-determinacy of GR is resolved by the choice of coordinates conditions. Here, one needs to impose some gauging conditions to define the scale factor λ. The term $\lambda^2\Lambda_E$ represents the energy density of the empty space in the scale-invariant context and we made the specific hypothesis that *the properties of the empty space, at macroscopic scales, are scale-invariant* (Maeder 2017a).

This choice is justified since the usual equation of state for the vacuum $P_{vac} = -\rho_{vac}$ is precisely the relationship that is permitting ρ_{vac} to remain constant for an adiabatic expansion or contraction (Carroll et al. 1992). At the quantum level, this does not necessarily apply, however in the same way as one may use Einstein's theory at large-scales, even if it does not apply at the quantum level, we do consider that the large-scale empty space is scale-invariant. Under the above key hypothesis one is left with the following condition for empty "vacuum" spacetime deduced from the field equation (18):

$$\kappa_{\mu;\nu} + \kappa_{\nu;\mu} + 2\kappa_\mu\kappa_\nu - 2g_{\mu\nu}\kappa^\alpha_{;\alpha} + g_{\mu\nu}\kappa^\alpha\kappa_\alpha = \lambda^2\Lambda_E\,g_{\mu\nu}. \quad (23)$$

Now, with the assumption that λ is only a function of t, required by considerations of space homogeneity and isotropy, one obtains the non-zero terms κ_0 and $\dot\kappa_0$ and with Equation (9) one has $\kappa_0 = -\dot\lambda/\lambda$, (dots indicating time derivatives). Thus, the above condition (23) leads to (Maeder 2017a)

$$3\frac{\dot\lambda^2}{\lambda^2} = \lambda^2\Lambda_E \quad \text{and} \quad \frac{\ddot\lambda}{\lambda} = 2\frac{\dot\lambda^2}{\lambda^2}, \quad (24)$$

which show similarity with de Sitter cosmological model, however here these equations establish a relation between the scale factor λ and Λ_E, which means that the scalar field λ, κ_ν, and the cosmological constant are closely related. In GR, Λ_E and thus the properties of the empty space are considered to not depend on the matter content of the Universe. We adopt the same assumption here. This means that the above relations (24) are always valid, whatever the matter content. According to discussions by Maeder (2017a) and Maeder and Gueorguiev (2019), their solution is of the form - the cosmic time gauge:

$$\lambda = \frac{A}{t}, \quad (25)$$

where $A = \sqrt{\frac{3}{\Lambda_E}}$ follows from the first equation. Equations (24) lead to considerable simplifications in the cosmological equations derived by Canuto et al. (1977) leading to solutions different, but no too far from the ΛCDM models. These models compare remarkably well (Maeder 2017a) with cosmological observations showing an acceleration of the cosmic expansion.

4   THE RADIAL ACCELERATION RELATION IN THE SCALE-INVARIANT VACUUM THEORY

4.1   The weak-field equation in the Scale-Invariant Vacuum theory

The equivalent of the Newton equation in the scale-invariant framework was derived from the weak-field approximation of the geodesic equation (Maeder & Bouvier 1979; Maeder 2017c). This geodesic equation follows from an action principle discussed in Dirac (1973), see also Bouvier & Maeder (1978). The equation of motion in spherical coordinates is:

$$\frac{d^2\vec{r}}{dt^2} = -\frac{GM}{r^2}\left(\frac{\vec{r}}{r}\right) + \kappa(t)\frac{d\vec{r}}{dt}. \quad (26)$$

From Equations (9) and (25), the coefficient of metrical connection has the simple form $\kappa(t) = 1/t$, where in the weak field approximation t is the cosmic time. In the case of the two-body problem, in radial coordinates where the trajectory is viewed as a segment of a circle with a radius $r(t)$, the correction term is proportional to the tangential velocity $\vec{v} = d\vec{r}/dt = \vec{\omega} \times \vec{r}$ where $\vec{\omega}$ is the corresponding angular velocity vector. In this framework, the radial component of the gravity is due to the usual Newtonian term and has no contribution from the correction term related to $\kappa(t)$. The effect of the correction term is only on the tangential component of the motion. As discussed for the 2-body problem (Maeder & Bouvier 1979; Maeder 2017c), this leads to a secular increase of the orbital radius, the circular velocity keeping constant. For a general non-circular motion, (26) shows an overall enhancement to the radial motion. That is, an outgoing motion gets an extra boost outwards and similar for an in-falling motion which is accelerated inwards. The effect is strongly reduced at the current age of the Universe. For the early Universe, however, this enhanced flow results in much faster structure formation (Maeder and Gueorguiev 2019).

One easy way to see where the extra term in the equation (26) is coming from is to extend the notion of parallel transport as defined by the equation of the geodesics. It has been proven in Bouvier & Maeder (1978) that the generalized equation of the geodesics follows from a unique action functional build from the length function of power (-1). Thus, by extending the usual equation of the geodesics from the Einstein GR space to the Weyl integrable space with modified Christoffel symbols (15) and turning the standard covariant derivative ";" into co-covariant derivative "*" one has $u^\nu u^\mu_{;\nu} = 0 \rightarrow u^\nu u^\mu_{*\nu} = 0$. Based on the definitions in (15) and (14) this becomes:

$$u^\nu u^\mu_{*\nu} = u^\nu u^\mu_{;\nu} + u^\nu[(g_{\nu\alpha}\kappa^\mu - g^\mu_\nu \kappa_\alpha - g^\mu_\alpha \kappa_\nu)u^\alpha - n\kappa_\nu u^\mu] = 0,\tag{27}$$

$$u^\nu u^\mu_{*\nu} = u^\nu u^\mu_{;\nu} + (u \cdot u)\kappa^\mu - (2+n)(u \cdot \kappa)u^\mu = 0.\tag{28}$$

This expression shows that for a co-vector u^μ of power -1 ($n = -1$) within the gauge choice for κ_ν (9) with $\lambda(t)$ satisfying (24) the usual weak-field geodesic equation will have an additional term that will look like an external force of the form $u^0 \kappa_0 u^i$. That is, $u^\nu u^i_{*\nu} = 0 \Rightarrow u^\nu u^i_{;\nu} = u^0 \kappa_0 u^i$. Here $i = 1, 2, 3$ is indexing the spacial components of the four-vector u. Since the three dimensional velocity can be expressed as $v^i = dx^i/dt = c\,dx^i/dx^0 = cu^i/u^0$, one is arriving at (26).

In what follows, we will try to estimate the magnitude of the ratio of the correction term $\kappa(t)\,v$ to the usual Newtonian term:

$$x = \frac{\kappa\,v\,r^2}{GM}.\tag{29}$$

Note that $x \approx 0$ corresponds to negligible corrections to the Newton's equation and thus in this case perturbation methods can be used, while $x \approx 1$ and bigger is the strong corrections regime. Because $\kappa(t)$ and the Hubble constant $H(t) = \dot{a}/a$ are co-scalars of rank (-1), therefore $H(t)/\kappa(t)$ is in-scalar, that is independent of the general scale factor λ. Since in normalized cosmic time units $t = t_0 = 1$ then one has $\kappa(t_0) = 1$ and $H(t_0) = 2$ in the absence of matter (see the

discussion after eq. 32 in Maeder and Gueorguiev (2019)); thus, $H(t)/\kappa(t) = 2$ in the totally empty flat universe.

In general, $\xi = H(t)/\kappa(t) = H(\tau)/\kappa(\tau) = H(t_0)/\kappa(t_0) = 2\left(1 - \Omega_{\mathrm{m}}^{1/3}\right)/(1 - \Omega_{\mathrm{m}})$. For $\Omega_{\mathrm{m}} = 0.30, 0.20, 0.10, 0.04$ one gets $\xi = 0.944, 1.038, 1.191$ and 1.371 respectively, which are all of order 1. This way the ratio x is:

$$x = \frac{\kappa\,v\,r^2}{GM} = \frac{H_0}{\xi}\frac{v\,r^2}{GM}.\tag{30}$$

By using the expression of the Hubble constant H_0 via the critical density $\rho_c = 3H_0^2/(8\pi G)$, along with the mean mass density $\overline{\rho}$ of the total mass M within a sphere with a radius R (defined as usual to be $\overline{\rho} = 3M/(4\pi R^3)$) one has:

$$x = \frac{\sqrt{8\pi G\rho_c/3}}{\xi}\frac{v}{G}\left(\frac{3r^2}{4\pi R^3\overline{\rho}}\right) = \frac{\sqrt{2}}{\xi}\left(\frac{\rho_c}{\overline{\rho}}\frac{v^2 r^2}{GR^3}\right)^{1/2}\left(\frac{3r^2}{4\pi R^3\overline{\rho}}\right)^{1/2},\tag{31}$$

This expression can be written also in the following form:

$$x = \frac{\sqrt{2}}{\xi}\left(\frac{\rho_c}{\overline{\rho}}\frac{v^2 r}{GM}\right)^{1/2}\left(\frac{r^3}{R^3}\right)^{1/2}.\tag{32}$$

When the radius of the sphere R defining the mean mass density $\overline{\rho}$ coincides with r, which is a consistent choice, one obtains:

$$x = \frac{\sqrt{2}}{\xi}\left(\frac{\rho_c}{\overline{\rho}}\frac{v^2 R}{GM}\right)^{1/2} = \frac{\sqrt{2}}{\xi}\left(\frac{\rho_c}{\overline{\rho}}\frac{g_{obs}}{g_{bar}}\right)^{1/2},\tag{33}$$

where $g_{\mathrm{obs}} = v^2/r$ is the kinematic rotational acceleration in circular motions, and $g_{\mathrm{bar}} = GM/r^2$ is the acceleration due to the mass present within the radius considered. The above expression (33) only applies to spherical distributions of matter.

In the standard Newtonian gravity one usually has $v^2 r = GM$ which results in:

$$x = \frac{\sqrt{2}}{\xi}\left(\frac{\rho_c}{\overline{\rho}}\right)^{1/2}.\tag{34}$$

This is the expression of the x-ratio when the deviations from the Newtonian case are small ($x \ll 1$) with an average matter density much bigger than the critical density, $\overline{\rho} \gg \rho_c$. A similar expression was used in Maeder (2017c) for the discussion of clusters of galaxies.

4.2 The radial acceleration relation (RAR) within the SIV context

The radial acceleration relation (RAR) expresses the relation between quantities $g_{\mathrm{obs}} = v^2/r$ and $g_{\mathrm{bar}} = GM/r^2$, *i.e.* between the kinematic rotational acceleration in circular motions and the acceleration due to the mass present within the radius considered (McCaugh et al. 2016; Lelli et al. 2017). In the Newtonian context, g_{obs} and g_{bar} are expected to be equal.

Let us start with Equation (30) written as:

$$x = \frac{H_0}{\xi}\frac{(r\,g_{\mathrm{obs}})^{1/2}}{g_{\mathrm{bar}}}.\tag{35}$$

Quite generally, the ratio x is a function $x(r,t)$ of space and time. At a given time, one has for the spatial dependence:

$$x(r) \sim \frac{(r\,g_{\mathrm{obs}})^{1/2}}{g_{\mathrm{bar}}}.\tag{36}$$

As a result of the time evolution of the system in the scale-invariant context, there is a difference between the two accelerations $g_{obs}(r,t)$ and $g_{bar}(r,t)$ at a given location. Let us write it as $g_{obs} = g_{bar} + \Delta g$. From the meaning of x encoded in its definition via Equation (26), x is the ratio of the difference between the total acceleration and g_{bar} with respect to g_{bar}. Since the motions in spiral galaxies are essentially circular, the main component of the total acceleration is still g_{obs}, the centripetal acceleration. Indeed, for the Sun the value of the circular velocity is 248.5 km s^{-1}, the radial component 13.0 km s^{-1} and the "vertical one" 7.84 km s^{-1} (Schoenrich 2012). Thus, one can write:

$$x(r) \approx \frac{\Delta g}{g_{bar}}. \tag{37}$$

From expressions (36) and (37), one has the relation,

$$\frac{g_{obs} - g_{bar}}{g_{bar}} \sim \frac{(r\, g_{obs})^{1/2}}{g_{bar}}. \tag{38}$$

In order to eliminate the proportionality factor in Equation (38), one can consider two gravitational systems 1 and 2 with respective baryonic gravities $g_{bar,1}$ and $g_{bar,2}$, observed at the same time t and coordinate r, with dynamical gravities $g_{obs,1}$ and $g_{obs,2}$. The ratio of the relative differences $\left(\frac{g_{obs}-g_{bar}}{g_{bar}}\right)$, should according to (38) behave like:

$$\frac{\left(\frac{g_{obs}-g_{bar}}{g_{bar}}\right)_2}{\left(\frac{g_{obs}-g_{bar}}{g_{bar}}\right)_1} = \left(\frac{g_{obs,2}}{g_{obs,1}}\right)^{1/2} \left(\frac{g_{bar,1}}{g_{bar,2}}\right). \tag{39}$$

The r-dependence simplifies when the gravities are considered at the same location in the two systems. This means that the two systems differ by the importance of their central mass and/or by their density distribution. This equation can also be written as:

$$\left(\frac{g_{obs}}{g_{bar}}\right)_2 = 1 + \frac{g_{bar,1}}{g_{bar,2}} \left(\frac{g_{obs,2}}{g_{obs,1}}\right)^{1/2} \left[\left(\frac{g_{obs}}{g_{bar}}\right)_1 - 1\right]. \tag{40}$$

This expression relates the values of a particular gravitational system 2 to those of another system 1, chosen as a reference at the same time t and location r. The nature of this reference is discussed below.

We now move to notations often used in the MOND context (Milgrom 2019), there g_{obs} is just g and g_{bar} is the Newtonian gravity g_N. We can write Equation (40) in a compact form:

$$\frac{g}{g_N} = 1 + \left(\frac{g^{1/2}}{g_N}\right) k_1 (k_2 - 1), \tag{41}$$

$$\text{with } k_1 = \left(\frac{g_N}{g^{1/2}}\right)_1, \text{ and } k_2 = \left(\frac{g}{g_N}\right)_1.$$

which is:

$$\frac{g}{g_N} = 1 + k \left(\frac{g^{1/2}}{g_N}\right), \quad \text{with } k = k_1(k_2 - 1) = \left(\frac{g - g_N}{\sqrt{g}}\right)_1. \tag{42}$$

We see that the k-term only depends on the reference system 1 and that $(k_2 - 1)$ cannot be equal to strictly zero since in any dynamical situation the additional acceleration term in Equation (26) is always present and therefore $k_2 > 1$, thus, k is also positive. Equation (42) is a second-degree polynomial equation,

$$g^2 - g(2g_N + k^2) + g_N^2 = 0, \tag{43}$$

with two solutions:

$$g = g_N + \frac{k^2}{2} \pm \frac{1}{2}\sqrt{4g_N k^2 + k^4}. \tag{44}$$

Equation (43) can be derived directly from (38). In this case (35) will provide the following expression for $k^2 \approx H_0^2 R$. We will come back to this expression in our estimate of k^2 as discussed in (54). The advantage of using (39) is the obvious scale invariance of the expression. In this respect there are two scale-invariant solutions as seen in (44). The sign "+" should be chosen since g is generally found larger than g_N.

There are two limiting cases predicted by this equation. First, we have the case where the Newtonian gravity most largely dominates over the effects due to scale invariance,

$$g_N \gg k^2, \quad \text{then } g \to g_N, \tag{45}$$

the dynamical gravity v^2/r tends towards the baryonic gravity GM/r^2. Indeed, as the equations (39) and the following ones concern the relations of g_{obs} with g_{bar} for given values of the radii, this means that very large values of g_{bar} are due to very large masses. Thus, this case occurs for a very large central mass and/or a high internal density distribution. Notice that expression (44) may be simplified for gravities g_N much larger than k^2. There, Equation (44) can be approximated by

$$g \to g_N + \sqrt{g_N k^2}. \tag{46}$$

This approximation is valid when g_N is at least about two orders of magnitude larger than k^2.

The second interesting case occurs when g_N tends towards zero. This may occur at any value of r due to a vanishing central mass or to an extremely faint density distribution. In this case, the dynamical gravity g tends towards a limiting value k^2,

$$g_N \to 0, \quad \text{then } g \to k^2. \tag{47}$$

Thus, k^2 appears as a kind of residual background acceleration in the Universe, in the absence of significant local gravity. As the value of k^2 is obtained everywhere for the same limit $g_N \to 0$, we may consider that k^2 is the same everywhere. The well-defined RAR by Lelli et al. (2017), which concerns measurement points for different radii and inner masses, also indicates that a change of Newtonian gravity, due to mass or distance, results in similar effects.

Finally, we recall that we have considered galaxies at the same time, e.g. the present time, this is correct since the sample studied (Lelli et al. 2017) is formed of local galaxies. The value of the limiting constant k^2 needs to be estimated, we propose to determine it from observations as discussed in the next section.

4.3 An alternative demonstration of the basic equation

An alternative way to arrive at the relationship (36) in a more general setting can be obtained by the following reasoning. As it is well known from kinematics, the total acceleration of a massive object can be decomposed in tangential a_t acceleration along the trajectory of the object and a normal $a_n = v^2/r$ acceleration perpendicular to the instantaneous trajectory segment that can be viewed as part of an arc from a circle of radius r. Considering that the SIV

equation (26) predicts an extra acceleration that is along the trajectory of the object, then the following expression can be written:

$$\vec{g} = a_n \vec{e_n} + a_t \vec{e_t} = \frac{v^2}{r} \vec{e_n} + \frac{v}{t} \vec{e_t}, \qquad (48)$$

here $\vec{e_n}$ and $\vec{e_t}$ are the corresponding unit co-moving directional vectors. From Newtonian dynamics point of view the total acceleration of a massive object in a gravitational field would be:

$$\vec{g} = g_N \vec{e_R} + g_X \vec{e_X} = \frac{GM}{R^2} \vec{e_R} + g_X \vec{e_X} \approx \frac{G(M + M_X)}{R^2} \vec{e_R}, \quad (49)$$

here $\vec{e_R}$ is the corresponding unit vector pointing from the center of mass of the system to the object under consideration that is at a distance R, while g_X and $\vec{e_X}$ represent possible fictitious acceleration and its direction. In GR as well as in Newtonian mechanics the fictitious accelerations can be made to be zero upon a suitable choice of coordinates for the observer. Within the dark matter paradigm g_X is just due to an extra dark matter M_X component while the directions $\vec{e_R}$ and $\vec{e_X}$ are expected to coincide.

By looking at the magnitude of the total acceleration $\vec{g}$ via (48) and upon a simple rearrangement of the relevant terms along with the assumption $g_{obs} \approx a_n$ one can write:

$$x^2 = \frac{g^2}{g_N^2} - \left(\frac{a_n}{g_N}\right)^2 = \frac{(g - a_n)(g + a_n)}{g_N^2} \approx \frac{2a_t g_{obs}}{g_N^2}, \qquad (50)$$

where a_t is the magnitude of the tangential acceleration during the motion of a test particle. The above form leads to expression similar to (38). Thus, upon further applying the reasoning from Equation (38) to (42), this results in similar functional forms like (42) and subsequent expressions,

$$\frac{g}{g_N} = 1 + k \left(\frac{g^{1/2}}{g_N}\right), \quad \text{with } k^2 = 2a_t, \qquad (51)$$

where k^2 can be related to $2a_t$ as in (50) above. In this respect, k^2 is model (system) dependent acceleration; it has something to do with SIV theory as can be seen from its $2a_t$ form; it also has something to do with the state of the Universe at large cosmic scales, as mentioned above. Furthermore, notice that (49) does not seems to result in a relationship of the form (51) because the extra acceleration g_X is co-linear with the baryonic acceleration g_N, therefore, dark matter models are incapable of the universal behavior (51) as illustrated in what follows.

Notice that the expression in (37) has been shown to result in two identical mathematical expressions (42) and (51) with two potentially different interpretations of the constant k^2. The expression (42) is based on the comparison to a reference system for the purpose of eliminating the proportionality factor in (38), while (51) does not involve a reference system. However, both expressions are about the deviation from the Newtonian behavior and show that far from the central mass and/or in low-density regime the dynamical acceleration tends towards an asymptotic value k^2 that demonstrates a non-Newtonian regime. If this value is to be the same for both mathematical expressions (42) and (51) then one can conclude that $\kappa v \approx (\frac{H_0}{\xi})^2 r$, which is based on (35) and (50), that is apparently correct due to the definition of ξ and the role of H_0 in relating v and r.

In MOND it is assumed that the relation between the gravities g and g_N is a fundamental law. We do not assume the same in the scale-invariant theory. In the SIV framework, the fundamental law is Equation (26) obtained in the weak-field Newtonian-like approximation of the theory. Relation (44) is its application that is describing the connection between v^2/r and GM/r^2 for the conditions considered.

5 COMPARISON OF THEORIES AND OBSERVATIONS

5.1 The radial acceleration relation

We examine the radial acceleration relation (RAR) studied by McCaugh et al. (2016) and Lelli et al. (2017) for a sample of 240 galaxies of various morphological types. The relation between $\log g_{obs}$ and $\log g_{bar}$ over 6 dex in g_{bar}, from very massive galaxies to the faint dwarf spheroidals, is shown in Fig. 1. As stated by Lelli et al., when the baryonic contribution is measured, the rotation curve follows and reciprocally. For high gravities, the two gravities are equal, as predicted by the Newton Law. Below a value g_{bar} of about 10^{-10} m s^{-2}, the RAR significantly deviates from the 1:1 line, g_{obs} being larger than g_{bar}. These deviations are currently attributed to dark matter.

Within the context of the ΛCDM models of galaxy formation, the dark-matter description is made in terms of different mass-dependent density profiles of DM haloes (Di Cintio and Lelli 2016). SIV and MOND make sufficiently specific predictions that are testable against the observational data. One may also be able to test a large class of Extended Theories of Gravity (Capozziello & de Laurentis 2011) against the observational data, however, such models are often funneled into MOND relevant versions (Bernal et al. 2011).

We see in Fig. 1, as was also pointed out by Lelli et al. (2017), that the faint dwarf spheroidal galaxies seem to tend on the average towards a limiting asymptotic value of $\log g_{obs}$, when fainter object of lower and lower values of $\log g_{bar}$ are considered. There is clearly a large scatter in the observations of the dwarf spheroidals, particularly of the ultra-faint ones that were recently discovered and where often few stellar velocities are measured, making the average g_{obs} uncertain. However, some of these dwarf galaxies also contain several hundreds or even thousands of stars measured, for example, as in Fornax, Sextans, and Sculptor where their dynamics are well studied, see for example Strigari et al. (2018). In Section 5.2, the statistics of the asymptotic limit of the observed value of $\log g_{obs}$ is further analyzed.

Equation (44) also predicts a constant limiting value k^2 for the very low gravities, as shown by its limit (47). We propose to identify this constant k^2 with the observed limiting value of g_{obs} in the RAR given by Lelli et al. (2017). Fig. 1 suggests a value of $\log g_{obs}$ of about -10.85 for this limit, g_{obs} being expressed in m s^{-2}. This corresponds to a value of $k^2 = 1.41 \cdot 10^{-11}$ m s^{-2}. With this value of k^2, Equation (44) is fully determined. Table 1 shows the expected values of $\log g$ for different values of $\log g_N$ according to this equation, the corresponding values of MOND are also given according to the data indicated in the caption.
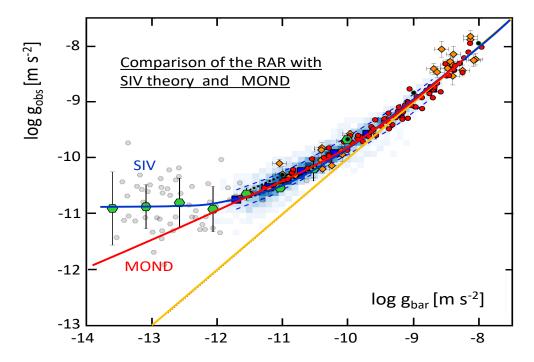
Figure 1. Observed values of g_{obs} and g_{bar} for the 240 galaxies studied by Lelli et al. (2017), forming the radial acceleration relation (RAR). The big green hexagons represent the binned data of the dwarf spheroidal galaxies which satisfy the three quality criteria of Lelli et al. (2017). The blue curve shows the relation predicted by expression (44) and given in Table 1 for SIV with a value of $k^2 = 10^{-10.85}$ m s^{-2}. The red curve gives the MOND relation from relation (56), with $a_0 = 1.20 \cdot 10^{-10}$ m s^{-2}, while the orange curve shows the 1:1-line.

Table 1. Values of $\log g_{obs}$ (or $\log g$) as a function of $\log g_{bar}$ (or $\log g_N$) in the SIV theory from (44) for $k^2 = 10^{-10.85}$, and in MOND from expression (56) with $a_0 = 1.20 \cdot 10^{-10}$, all accelerations being expressed in m s^{-2}.

	SIV	MOND
$\log g_{bar}$	$\log g_{obs}$	$\log g_{obs}$
-8.0	-7.984	-8.000
-9.0	-8.948	-8.975
-10.0	-9.838	-9.777
-11.0	-10.510	-10.399
-12.0	-10.794	-10.941
-13.0	-10.844	-11.454
-14.0	-10.849	-11.958

Fig. 1 compares the relation in Table 1 with the values of $\log g_{obs}$ and $\log g_{bar}$ for the 240 galaxies studied by Lelli et al. (2017). The SIV predictions remarkably agree with observations on the whole range of 6 dex in the accelerations and also produces the asymptotic behavior observed for dwarf spheroidal galaxies. The dynamical predictions of the scale-invariant theory, as expressed by the modified equation of mechanics (26), provides an account of the apparent excess of stellar velocities in galaxies, with respect to the mass present in them. The excellent agreement also concerns the spheroidal galaxies as analyzed by Lelli et al. (2017), which describes the RAR over such a large range of accelerations. This is quite interesting since these are the objects where the ratio of dark matter to baryonic matter is the highest, reaching up a factor 1000 (Sancisi 2004). Further analysis of the spheroidals is made in Section 5.2 below. For now, the general agreement found here is one more indication in

favor of the scale-invariant theory, also supported by the dynamics of cluster of galaxies, the flat galactic rotation curve, the absence of the flat curve in high redshift galaxies, the growth of the stellar velocity dispersions with ages (Maeder 2017c), as well as the growth of the density fluctuations in the early Universe (Maeder and Gueorguiev 2019), and half a dozen of basic cosmological tests (Maeder 2017a).

5.2 The asymptotic limit of the dwarf spheroidals

The asymptotic limit of dwarf spheroidal galaxies found by Lelli et al. (2017) needs to be further examined. A list of 62 dwarf spheroidals in the Local Group has been given by these authors, with luminosities, half-light radii, ellipticities, mean velocity dispersions, number of stars used to estimate the velocity dispersion, two gravity parameters $\log g_{bar}$ and $\log g_{obs}$ (this last one being estimated on the basis of the velocity dispersion). As mentioned by these authors, robust estimates of g_{obs} in dwarf spheroidals (dSphs) can only be made near the half-light radius, where the effects of anisotropy are small, however, there is an important exception in the case of the Fornax and Sculptor dwarf galaxies, which count respectively 2483 and 1365 stars measured (see below). Lelli et al. consider three quality criteria to retain or reject dSphs:

  (i) An ellipticity smaller than 0.45.
  (ii) Limited tidal effects from the host galaxy.
  (iii) The number N of stars with velocity measurements in a given galaxy. They retain only galaxies with $N > 8$.

The mean values obtained by Lelli et al. are represented by the green hexagons in Fig. 1 and define a flat asymptote at about $\log g_{obs} = -10.85$.
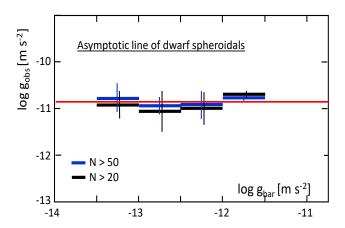
Figure 2. The mean value of $\log g_{\mathrm{obs}}$ per interval of $\log g_{\mathrm{bar}}$ for dwarf spheroidals. The horizontal red line represents the observed value of the asymptotic limit of the dwarf spheroidal galaxies in Fig. 12 by Lelli et al. (2017). The thick blue horizontal lines represent the mean over the interval of $\log g_{\mathrm{bar}}$ considered for galaxies with a number of observed stars $N \geq 50$, in black the average for galaxies with $N \geq 20$ are shown. The thin vertical bars shows the dispersions.

As the above number N is rather small, we now consider dwarf spheroidals that have a number N of measurements equal or larger than 20, and as another option those with $N \geq 50$. There are 38 dSphs of the first group and 16 of the second in the domain considered of $\log g_{\mathrm{bar}} \leq -11.50$. Fig. 2 shows the mean values in four intervals, with the error bars. For values of g_{bar} varying by a factor of 100, the value of g_{obs} remains constant. These two different samplings of spheroidals with a high number of stars measured confirm the results of Lelli et al. (2017), with the clear conclusion that whatever the sampling, the value of $\log g_{\mathrm{obs}}$ is about constant over an interval of 2 dex below about $\log g_{\mathrm{bar}} = -11.50$.

In this context, where several uncertainties are remaining, it is worth considering another test. The very rich dwarf galaxies Fornax and Sculptor show two chemo-dynamically distinct stellar components. They both have metal-poor (MP) and metal-rich (MR) stars, the MP stars (likely the older ones) being more broadly distributed than the more concentrated MR stars (Tolstoy et al. 2004; Battaglia et al. 2006). In these two galaxies, the MP and MR stars define two different half radii and the velocity dispersions of the two subgroups are different, nevertheless the values of g_{obs} are the same. As noted by Lelli et al. (2017): "Velocity dispersions and half-light radii seem to conspire to give a constant g_{obs}, in line with the apparent flattening of the relation at low g_{bar}". On the whole, the existence of the asymptotic flat line defined by the dwarf spheroidals appears as well supported.

5.3 On the significance and value of the acceleration term k^2

From Equations (41) and (42), the parameter k may be expressed in the following form:

$$k = k_1(k_2 - 1) = \left(\frac{g_{\mathrm{N}}}{g^{1/2}} \left(\frac{g}{g_{\mathrm{N}}} - 1 \right) \right)_1 = \left(\frac{g - g_{\mathrm{N}}}{g^{1/2}} \right)_1 . \quad (52)$$

The above relation is evidently consistent with the definition given by (42). It also shows that if g_{N} tends towards zero, then the dynamical gravity g would tend to k^2. Thus, k^2 appears as a background limiting value of the dynamical gravity for vanishing Newtonian gravity, independently of the radius considered. The origin, in the Newtonian approximation of the scale-invariant theory, of a non-vanishing dynamical gravity k^2, arises from the additional acceleration term in Equation (26). The accumulated effect of this term over the ages, with the assumption that the galaxies have the same age, leads to the resulting acceleration term. Physically, in the very faint systems (with $g_{\mathrm{N}} \to 0$), this background dynamical acceleration manifests itself as a velocity dispersion becoming larger at larger radii (leading to a constant acceleration), a behavior that is illustrated by the two chemically different components of the dwarfs Fornax and Sculptor.

Thus, the value of the background acceleration, k^2 is logically related to some cosmological properties of the Universe, in particular to the average matter density and its fluctuations. A detailed estimate is beyond the scope of the present paper, however, we may try to estimate the order of magnitude of k^2. The dynamical gravity is always larger or equal to the Newtonian gravity, thus when $g_{\mathrm{N}} \to 0$, we may expect that,

$$k^2 \to min[g_{\mathrm{N}}] = min\left[\frac{GM}{R^2} \right] = min\left[\frac{4\pi}{3} G \overline{\rho} R \right] . \quad (53)$$

For the density, we take the mean density of the Universe $\rho_{\mathrm{m}} = \Omega_{\mathrm{m}} \rho_{\mathrm{c}}$, with the critical density $\rho_{\mathrm{c}} = 3H_0^2/(8\pi G)$. Notice that these expressions result in $min[g_{\mathrm{N}}] \approx H_0^2 R$ that is also the mathematical relation for k^2 as discussed earlier in the paragraph after Eq. (44). For R, some fraction f of the Hubble scale c/H_0 is reasonable. Thus, one obtains the following estimate:

$$k^2 \approx \frac{1}{2} f \Omega_{\mathrm{m}} c H_0 . \quad (54)$$

Thus, the value of the minimum average acceleration k^2 is logically related to some cosmological properties of the Universe, in particular to the average matter density. Interestingly enough, k^2 depends on the constant c multiplied by the present expansion rate H_0, a dependence also present in the acceleration term a_0 of MOND (Milgrom 2009, 2015). Here in (54), there is a factor f necessarily smaller than one, which thus leads to a value of k^2 lower than the MOND parameter a_0, because the equations are also different. Furthermore, the above expression (54) implies that the minimum average dynamical acceleration would vanish only for an empty Universe.

The result above is consistent with a simple dimensional argument based on Equations (50) and (51) which shows that k^2 can be linked to the tangential acceleration $a_{\mathrm{t}} = v/t$ in the case of a specific object on cosmological scales. An

upper-value estimate of k^2 based on a_{t} as linked to the large scale cosmology parameters results in:

$$k^2 \sim a_{\mathrm{t}} = \upsilon/t = (H_0 R_{\mathrm{lim}})/t_0 = (H_0 c t_0)/t_0 = H_0 c, \qquad (55)$$

where t_0 is the age of the Universe. This way, we may understand the general dependence on cH_0, while the above estimate (54) contains a factor f smaller than 1 and demonstrates the influence of the total mass of the Universe within the past-causal cone of an arbitrary point that accounts for the matter density via the term Ω_{m}.

Let us examine numerically the approximation (54). We take a value of $H_0 = 70$ km s^{-1} Mpc^{-1}, thus $cH_0 = 6.801 \cdot 10^{-10}$ m s^2. For $\Omega_{\mathrm{m}} = 0.20$ or 0.30, we get $\frac{1}{2}\Omega_{\mathrm{m}} cH_0 = 6.80$ or 10.02 in units 10^{-11} m s^{-2} respectively. In Section 5.1, we considered the fact that k^2 could correspond to the asymptotic limit of the RAR with a value of $k^2 = 1.41 \cdot 10^{-11}$ m s^{-2}. This means that the numerical factor $f \approx 0.21$ or 0.14 respectively. This factor is evidently different, but not so much, from the ratio (0.18) of the MOND constant $a_0 = 1.20 \cdot 10^{-10}$ m s^2 to the product cH_0, since the equations are different. Nevertheless, as shown in the next Section, over a large range of gravities the two different approaches give the same numerical results.

Within the dark matter paradigm (49) the value of k^2, according to (52), is expected to be $k^2 = (g - g_{\mathrm{N}})^2/g = (GM_X/R^2)(M_X/(M + M_X))$ and in the limit $R \to R_{\mathrm{lim}}$ it becomes $k^2 = (g - g_{\mathrm{N}})^2/g \to GM_X/R_{\mathrm{lim}}^2 \times (\Omega_{\mathrm{DM}}/(\Omega_{\mathrm{b}} + \Omega_{\mathrm{DM}}))$, thus the factor Ω_{m} in (54) is replaced by $\Omega_{\mathrm{DM}}^2/(\Omega_{\mathrm{b}} + \Omega_{\mathrm{DM}})$ which is a dimensionless factor of $\Omega_{\mathrm{DM}}^2/\Omega_{\mathrm{m}}^2$ compared to $\Omega_{\mathrm{m}} = \Omega_{\mathrm{b}} + \Omega_{\mathrm{DM}}$. For ΛCDM baryonic matter fraction $\Omega_{\mathrm{b}} = 4\%$ and $\Omega_{\mathrm{DM}} = 25\%$ this will result in an factor of about $(25\%/29\%)^2 = 0.74$ which is ≈ 5 times bigger than the SIV value of k^2 given by (54). Furthermore, notice that (49) predicts $\log g - \log g_{\mathrm{N}} = \log(M_{\mathrm{tot}}/M_{\mathrm{bar}}) \approx \log 7 \approx 0.8$ that is a factor of 4 times smaller than what is seen in Fig. 3, which is most likely due to the fact that dark matter (49) cannot result in a relationship of the form (51).

5.4 Comparison and discussion

First, on the theoretical side, MOND is based on an hypothesis of scale invariance (Milgrom 2009), which assumes an invariance to space and time dilatations with a scale factor λ independent on time. This is a different and less general invariance than the SIV hypothesis, which assumes space-time invariance, with a scale factor $\lambda(t)$ dependent on time (see Sect. 2). Nevertheless, there is some proximity between the two. For example, in MOND, the orbital velocity around a bounded mass M becomes independent of the size of the orbit (Milgrom 2014). In SIV context, the circular velocity keeps constant during the secular increase of the orbital radius of a moving particle.

There is however an important question about MOND, which assumes a relation $a_0 \sim cH_0$ between the so-called "MOND fundamental constant" a_0 and the Hubble constant H_0. This raises the question of what happens to this relation at other epochs. We must logically wonder whether these "constants" do not depend on time as is the case for the expansion rate $H(z)$. If this is the case, this would clearly favor a variable scalar field, with a variable scale factor $\lambda(t)$, as assumed in the scale-invariant theory.

Keeping the previous notations, the expression of the acceleration of gravity in the MOND theory may be written as (Milgrom & Sanders 2008; Milgrom 2016),

$$g = \frac{g_{\mathrm{N}}}{\left[1 - e^{-(g_{\mathrm{N}}/a_0)^{\frac{1}{2}}}\right]}, \qquad (56)$$

an expression also used for example by McCaugh et al. (2016) and Dutton et al. (2019). There, the term a_0 represents a constant acceleration equal to about $a_0 = 1.20 \cdot 10^{-10}$ m s^{-2}. The MOND theory has two limits: first, for gravities $g_{\mathrm{N}} \gg a_0$, the dynamical gravity tends towards the Newtonian value g_{N}. The second limit is:

$$\text{for} \quad g_{\mathrm{N}} \ll a_0, \quad g \to \sqrt{g_{\mathrm{N}} a_0}, \qquad (57)$$

(Milgrom 1983, 2009, 2013, 2016). This is the so-called deep MOND limit for weak gravities. Several other overall expressions, different from Equation (56) have been considered over the years and they have been closely compared by Dutton et al. (2019). As one can see from (57), the MOND asymptotic limit of g related to vanishing baryonic gravity tends to zero. Thus, when g_N tends to zero so is g. In this respect, other RAR studies, such as that by Di Paolo et al. (2019), do not show the non-zero asymptotic limit of g when g_N tends to zero. In this case, a critical point may be that the stellar mass distribution "is estimated kinematically by means of mass modelling of the rotation curve". An explicit connexion between the velocity, the baryonic fraction and g_{bar} is used (see their Equation 7), while the g_{bar} estimates should be independent of velocity properties.

In the line of the mentioned proximity between MOND and the present work, it is interesting to compare the above low gravity limit in MOND as given by Equation (57) with the corresponding limit obtained in the SIV Equation (46). In both cases, there is a dependence on the square root of a product of g_{N} and a constant term. In MOND, this applies to the expression of g while in the SIV theory this applies to the difference $g - g_{\mathrm{N}}$. The constants are evidently different since the expressions are different, but the overall curves are very similar for about $\log g_{\mathrm{N}} > -11$, as illustrated by Figs. 1 and 3.

Let us estimate the differences $\Delta \log g = \log g - \log g_{\mathrm{N}}$ as a function of $\log g_{\mathrm{N}}$ for the two theories. Quantities $\Delta \log g$ represent the vertical deviations from the 1:1 line in Fig. 1. These deviations also correspond to $\log(\frac{M_{\mathrm{tot}}}{M_{\mathrm{bar}}})$, the log of the ratio of the total mass (including dark matter) to the baryons mass (Lelli et al. 2017). The values $\Delta \log g$ for the scale-invariant theory are based on the data of Table 1, for MOND they are obtained from Equation (56). These data are summarized in Table 2. The differences between the two remain very small at high accelerations, and thus the two theories are in excellent agreement down to $\log g_{\mathrm{N}} = -11.50$. However, for $\log g_{\mathrm{N}} \leq -12$, the differences become significant, the values of $\Delta \log g$ predicted by SIV theory becoming much larger than for MOND. This a consequence of the horizontal asymptote in Fig. 1, while at the lowest gravities the MOND curve continues to go down, as predicted by Equation (56) (Milgrom 2016).

The MOND theory can be recovered from the "$f(R)$-theories of Gravity" by Capozziello et al. (2006), already mentionned in Section 2. However, the $f(R)$ theories are more general than MOND, see also (Borka Jovanovic et al. 2016; Capozziello et al. 2017). According to these authors,
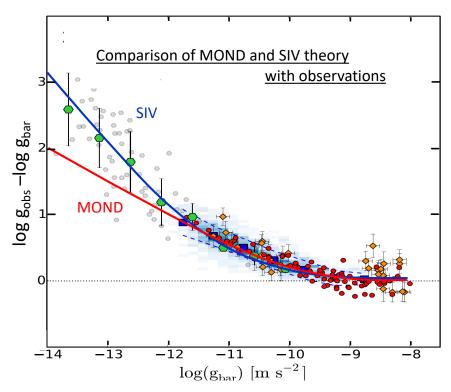
Figure 3. The observed deviations $\Delta \log g = (\log g - \log g_{\mathrm{N}})$ for the 240 galaxies analyzed by Lelli et al. (2017). The quantity $\Delta \log g$ is also equal to $\log(\frac{M_{\mathrm{tot}}}{M_{\mathrm{bar}}})$, the log of the ratio of the total mass (including the supposed dark matter) to the baryonic matter. The MOND and SIV model predictions are compared with the observations.

Table 2. Values of differences between $\log g$ and $\log g_{\mathrm{N}}$ for the scale-invariant vacuum theory and for MOND. The values for SIV are derived from Table 1 based on Equation (44), for MOND the values are obtained from Equation (56), with $a_0 = 1.20 \cdot 10^{-10}$ m s^{-2}.

$\log g_{\mathrm{bar}}$	$\Delta \log g$ SIV	$\Delta \log g$ MOND
-8.0	0.016	0.000
-9.0	0.052	0.025
-10.0	0.162	0.223
-11.0	0.490	0.601
-12.0	1.206	1.059
-13.0	2.156	1.546
-14.0	3.151	2.042

several issues of fundamental physics suggest that higher order terms must enter the gravity Lagrangian. Thus the action writes

$$A = \int d^4 x \sqrt{-g} \left[f(R) + \mathscr{L}_m \right], \tag{58}$$

where $f(R)$ is some function of the Ricci curvature scalar. Changing the gravity Lagrangian modifies the potential in the weak field approximation. The case $f(R) = R$ corresponds to GR. A power law $f(R) = f_0 R^n$ is often considered, with f_0 being some numerical constant. In this case, the resulting potential Φ takes a simple form, in which appears an additional fundamental radius r_{c} (in addition to the Schwarzschild radius). The corresponding velocity of circular motions becomes

$$v_{\mathrm{c}}^2(r) = \frac{GM}{2r} \left[1 + (1 - \beta) \left(\frac{r}{r_{\mathrm{c}}} \right)^{\beta} \right], \tag{59}$$

where the parameter β may depend on the scale of the objects considered. A value $n = 1$ and $\beta = 0$ applies to the Solar System, while from their velocities and luminosities, a value $\beta = 0.817$ is adopted for galaxies. For β between 0 and 1, the predicted velocities are larger than the standard values and thus this "may fill the gap between theory and observations without the need of additional dark matter" Capozziello et al. (2006). These authors show an excellent fit of the rotation curve with the rotation profiles (59) for the above parameter β. For a value of $n = 3/2$, the $f(R)$-theory converges to a MOND-like acceleration $a \simeq (a_o GM)^{1/2}/r$. There is also a relation between the MOND parameter a_0 and the new radius r_{c} according to Capozziello et al. (2017). These authors show an excellent agreement of their model with the baryonic Tully-Fisher relation, as MOND is doing. These developments well illustrate the variety of approaches of the Extended Theories of Gravity in order to account for the flat high rotation curves of galaxies

We now turn to the comparison with the observations. There are undoubtedly several successes of MOND in galaxy dynamics, making it a challenging theory to the ΛCDM models, as emphasized by McGaugh (2015). The comparison of MOND and SIV predictions is made in Fig. 3. Over the whole range from the large elliptical galaxies to the low mass spirals down to about $\log g = -11.50$, the agreement between the two curves, as well as with the observations is excellent.

It is only for extremely low gravities below the above value that the two theoretical curves disagree. At $\log g_{\text{bar}} = -13.50$, which corresponds to the lowest observed values, the ratio of g/g_{N} (or $M_{\text{tot}}/M_{\text{bar}}$) predicted by MOND is about 59 while that by SIV is 478, very close to the value supported by the observations. Thus, the MOND predictions and the observations of the dwarf spheroidals do not fit, a point also mentioned by Dutton et al. (2019). The dwarf spheroidals, which are the objects where the amount of dark matter with respect to baryons is the highest, appear to have a critical role in constraining theories. There are is still uncertainties in the relevant data, and thus observations of greater accuracy of dwarf spheroidals are very needed.

6 CONCLUSIONS

The SIV theory is based on the key hypothesis that the macroscopic empty space possesses a scale-invariant symmetry with respect to time and space. Within the Weyl Integrable Geometry, this results in a modified equation of motion (26). This equation leads to a specific relationship (38) between the observed kinematical acceleration $g_{\text{obs}} = v^2/r$ and the Newtonian acceleration due to baryonic matter $g_{\text{bar}} = GM/r^2$. The relationship is further explored in general terms and leads to the two-point correlation (40) which can be cast in the key expression (44). Alike MOND, SIV theory well accounts for the RAR down to $\log g_{\text{bar}} = -11.50$ as seen in Fig. 1. For lower gravities, SIV is still in full agreement, while this is not the case for MOND, e.g. the case of the dwarf spheroidals discussed above. Via (44) SIV predictions naturally accounts for the horizontal asymptotic limit (47) of the RAR relation, which corresponds to a minimum acceleration of about $\log(g) = -10.85$ (where g is expressed in m $\cdot$ s^{-2}). This empirical value, which critically depends on the dispersion velocities of dSph galaxies, appears stable with respect to a reasonable set of sampling selection choices as demonstrated by Fig. 2. A theoretical interpretation of this constant gives a reasonable agreement.

On the whole, the above results suggest, in addition to other tests such as the growth of the density fluctuations (Maeder and Gueorguiev 2019), that there is no need for dark matter and that the RAR and related dynamical properties of galaxies can be interpreted by a modification of gravitation, as proposed by the Scale-Invariant Vacuum theory.

ACKNOWLEDGEMENTS

REFERENCES

Battaglia, G., Helmi, A., Tolstoy, E. et al. 2008, ApJ, 459, 423

Bernal, T., Capozziello, S., Hidalgo, J. C., & Mendoza, S. 2011, European Physical Journal C, 71, 1794

Bondi, H. 1990, in Modern Cosmology in Retrospect, Eds. Bertotti, B., Balbinot, R., & Bergia, S.,Cambridge Univ. Press., 426 pp.

Bouvier, P. & Maeder, A. 1978, Ap&SS, 54, 497

Borka Jovanovic, V., Capozziello, S., Jovanovic, P. et al. 2016, Phys. Dark Univ, 14, 73

Canuto, V., Adams, P. J., Hsieh, S.-H., & Tsiang, E. 1977, Phys. Rev. D, 16, 1643

Capozziello, S., Cardone, V.F., Troisi, A. 2006, JCAP, 1706, 044

Capozziello, S., & Stornaiolo, C. 2008, International Journal of Geometric Methods in Modern Physics, 5, 185

Capozziello, S., & de Laurentis, M. 2011, Physics Reports, 509, 167

Capozziello, S., Jovanovic, P., Borka Jovanovic, V. et al. 2017, JCAP, 1706,044

Carroll, S. M., Press, W. H., & Turner, E. L. 1992, Annual Tev. Astron. Astrophys., 30, 499

Desmond, H. 2017, MNRAS, 464, 4160

Di Cintio, A., Lelli, F. 2017, MNRAS, 456, L127

Dirac, P. A. M. 1973, Proceedings of the Royal Society of London Series A, 333, 403

Dutton, A.A., Maccio, A.V., Obrera, A. et al. 2019, MNRAS 485, 1889

Di Paolo, C., Salucci, P., & Fontaine, J. P. 2019, ApJ, 873, 106

Eddington, A. S. 1923, The mathematical theory of relativity, Chelsea Publ. Co. New York, 270 p.

Faber, S. M. and Jackson, R. E. 1976, ApJ, 204, 668

Keller, B.W., Wadsley, J.W. 2017, ApJ, 835, L17

Kijowski, J. 2016, International Journal of Geometric Methods in Modern Physics, 13, 1640008-2924

Lelli, F., McGaugh, S.S., Schombert, J.M., Pawlowski, M.S., 2017, ApJ, 836, 152

Li, P., Lelli, F., McGaugh, S. et al. 2018, A&A, 615, A3, 70

Ludlow, A.D., Benitez-Lambay, A. Schaller, M. e al. 2017, PhRvL. 118,1103

Maeder, A. 2017a, ApJ, 834, 194

Maeder, A. 2017c, ApJ, 849, 158

Maeder, A., Bouvier, P. 1979, Astron. Astrophys., 73, 82

Maeder, A., Gueorguiev, V., G. 2019, Physics of the Dark Universe, 25, 100315

Massari, D., Breddels, M.A., Helmi, A. et al. 2017, Nature Astronomy, 2, 156

McGaugh, S.S. 2004, ApJ, 609, 652

McGaugh, S. 2015, Canadian Journ. of Physics, 93, 250

McGaugh, S.S., Lelli, F., Schombert, J.M. 2016, Phys. Rev. Lett. 117, id.201101

Milgrom, M. 1983, ApJ, 270, 365

Milgrom, M. 2009, ApJ, 698, 1630

Milgrom, M. 2013, Phys. Rev. Letters, 111, 041105 91

Milgrom, M. 2014, MNRAS, 437, 2531

Milgrom, M. 2015, Phys. Rev. D. 91, 044009

Milgrom, M. 2016, arXiv:1609.06642

Milgrom, M. 2019, Physicl Review D, 99, 044041

Milgrom, M., Sanders, R.H. 2008, ApJ, 678, 131

Navarro, J.F., Benitez-Llambay, A., Fattahi, A. et al. 2017, MNRAS, 471, 1841

Sancisi, R. 2004, IAU Symp. 220, Dark Matter in Gakaxies, ed. S. Ryder et al., p. 233

Santos-Santos, I.M., Brook, C.B., Stinson, G. et al. 2016, MNRAS, 455, 476

Strigari, L.E., Frenk, C.S., White, S.D.M. 2018, ApJ, 860, 56

Schoenrich, R. 2012, M.N.R.A.S. 427, 274

Tolstoy, E., Irwin, M.J., Helmi, A. et al. ApJ, 617, L119

Tully, R. B., Fisher, J.R. 1977, Astron. Astrophys., 54, 661

Walker, M.G.. Penarrubia, J. 2011, ApJ, 742, 20

Weyl, H. 1923, Raum, Zeit, Materie. Vorlesungen über allgemeine Relativitätstheorie. Re-edited by Springer Verlag, Berlin, 1970

This paper has been typeset from a TeX/LaTeX file prepared by the author.